

# Spin transfer torque effects in nanopillar devices with perpendicular anisotropy

S. Mangin

Institut Jean Lamour, Nancy-Université

Campus Aiguillettes BP 70239

Vandoeuvre-lès-Nancy F-54506, France

Phone: +33-(0)3-83 68 48 31 E-mail: stephane.mangin@ijl.nancy-universite.fr

## 1. Introduction

As predicted by L. Berger [1] and J. Slonczewski [2] when a current of polarized electrons enters a ferromagnet the current exert a torque on the ferromagnet magnetization. This torque can lead to magnetization switching between two stable configurations which was later demonstrated in nanopillar spin-valve structures [3-4]. The ability of a spin-polarized current to reverse the magnetization orientation of nanomagnets should enable a range of magnetic devices such as high performance random-access magnetic memory. However, several advances are needed to realize practical devices [5]. One key point is the reduction of the currents required to switch magnetization while maintaining the thermal stability of the free layer. Other key point are the control of the magnetic configurations and their dynamics

There have been a range of approaches to lower the switching currents by optimizing the materials properties, modifying the layer sequence or sample architecture [6-8]. In this paper we discuss the approach of using samples exhibiting perpendicular anisotropy a pathway to low critical current while maintaining large thermal stability

Since 2006 a few groups have focus their work on preparing nanopillar spin valve exhibiting perpendicular anisotropy [9-15]. Their motivation were both to give a deeper understanding of spin transfer torque in this geometry but also to test prediction that such system provide a pathway to low critical current. Seki *et al* have designed devices using perpendicularly magnetized FePt layers whereas Meng *et al* used [CoFe/Pt] multilayers. In the current paper we describe structures made of Co/Pt and Co/Ni multilayers with perpendicular magnetic anisotropy [9-11]. They were grown both by co-evaporation and DC magnetron sputtering. The magnetic structure shown in Fig. 1 consists of a Pt(3nm)/[Co(0.25 nm)/Pt(0.52 nm)]<sub>x4</sub>/Co(0.2 nm)/[Ni(0.6 nm)/Co(0.1 nm)]<sub>x2</sub>/Co(0.1 nm) hard reference layer and a Co(0.2 nm)/[Ni(0.6 nm)/Co(0.1 nm)]<sub>x4</sub>/Pt(3 nm) free layer separated by a 4-nm Cu spacer layer. After the film growth, the multilayers were patterned using electron beam lithography to provide nanopillars of different shapes (circle, square, hexagone and rectangle) and sizes (from 50 nm to 5 μm). In all those devices, the resistance of the device depends on its magnetic state, through the giant magnetoresistance effect, so that measuring the resistance of the structure allows the magnetic state to be inferred. All transport measurements are quasi-static and were performed using an AC-Bridge which gives a value of the differential resistance  $R_{AC} = dV/dI$ . The signature of a spin transfer effect is a change in the resis-

tance of the device that is asymmetric in the current.

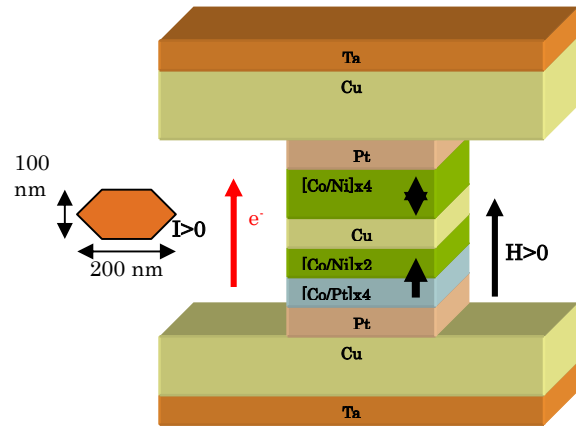


Fig.1: a) Schematic representation of a patterned perpendicular spin valve. The hard layer is a composite [Co/Pt]<sub>x4</sub>/[Co/Ni]<sub>x2</sub> multilayer and the free layer is a [Co/Ni]<sub>x4</sub> multilayer. The magnetization direction of the hard layer is parallel to the positive field direction. For positive current, the electrons are flowing from the hard layer to the free layer.

In the macro-spin approximation, the critical current for spin-transfer reversal of a free layer at zero temperature is given by

$$I_{C0} = -\left(\frac{2e}{\hbar}\right) \frac{\alpha M_S V}{g(\theta) p} H_{eff} \quad (1)$$

where  $M_S$  and  $V$  are the saturation magnetization and volume,  $\alpha$  is Gilbert's damping constant, and  $p$  is the spin polarization of the current. The factor  $g(\theta)$  depends on the relative angle  $\theta$  of the reference- and free-layer magnetization vectors.  $H_{eff} = (H_{K\perp} - 4\pi M_S + H_{app} + H_{dip})$  is the effective field acting on the free layer which contains contributions from the perpendicular applied field  $H_{app}$ , the dipolar field from the reference layer  $H_{dip}$ , and the uniaxial PMA field  $H_{K\perp}$ . The factor  $-4\pi M_S$  arises from the demagnetizing field of the thin film geometry.

The thermal stability of the free element is determined by the height of the energy barrier  $U_K = [M_S V (H_{K\perp} - 4\pi M_S)] / 2$  between the two stable magnetization configurations. Thus the critical current is directly proportional to the energy barrier in the absence of external field,  $H = H_{dip} + H_{app} = 0$ :

$$I_{C0} = -\left(\frac{2e}{\hbar}\right) \frac{2\alpha}{g(\theta)_p} U_K \quad (2)$$

Within the assumptions of Eq. 2, low critical currents can then be achieved by reducing the  $\tilde{\alpha}p$  ratio and minimizing  $U_K$ , while maintaining thermal stability. By adjusting the perpendicular anisotropy and volume of the free element consisting of a [Co/Ni] multilayer one can observe that the critical current scales with the height of the anisotropy energy barrier and critical currents as low as 120  $\mu$ A is achieved in quasi-static room-temperature measurements of a 45-nm diameter device [16]. To study the combined effect of an applied magnetic field  $H$  and a bias current  $I$  on the nanopillar spin-valve, the magnetoresistance response is measured in the  $(H, I)$  parameter space and  $H$  vs  $I$  phase diagrams were built. Several magnetization reversal dynamic could be identified (hysteretic magnetization reversal, magnetization precession, domain wall propagation).

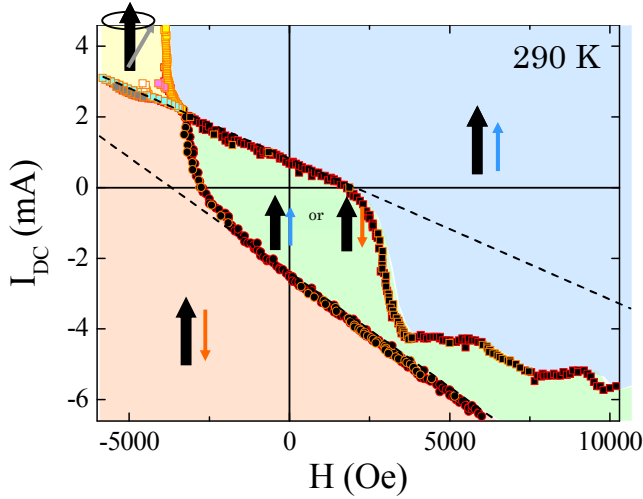


Fig.2: Experimentally determined  $(H, I)$  phase diagram for a 50 x 100 nm<sup>2</sup> hexagonal nanopillar at 290 K. In the blue region (1) the free and the hard layer magnetization are pointing along the positive field direction; It corresponds to the parallel state. Symmetrically, in the red region (2) the free layer magnetization is pointing along the negative field direction; This corresponds to the anti-parallel state. The green region (3) is a bistable region where the parallel and the antiparallel states are possible. In the yellow region (4), a precessional state is observed. The hysteretic reversals of the magnetization from the parallel state to the antiparallel state (resp. from the antiparallel state to the parallel state) are indicated by circles (resp. squares) filled with black. Symbols with red (resp. orange) edges correspond to transitions observed while sweeping the current  $I$  (resp. the field  $H$ ). Symbols filled with other colors indicate reversible changes in the device resistance.

The experimental phase was compared to the phase diagram calculated in the macrospin approximation. This phase diagram has been calculated by several authors in various approximation conditions see ref [17-18]. Most discrepancies between the measured and theoretical phase diagram could be explained considering the total effective field applying on the nanopillar soft layer [19].

The dynamic of the hysteretic behavior was studied. Pulses between 100 ps and 1 ms duration and amplitudes of up to 2 V were injected into the sample to determine the

switching probability for different external fields perpendicular to the plane. The results [20] are compared to theoretical models and calculation [21]

Finally domain walls can nucleate and propagate in perpendicularly magnetized nanopillar spin valves as small as 50 x 100 nm<sup>2</sup> [10]. The study of these domain walls is of great interest to enable new applications such as race track or multi-level memories [22]. Telegraph noise behaviour in nanopillars with perpendicular anisotropy has been reported [23]. For various injected current and different applied field telegraph noise was observed and studied. The probability of staying in a given magnetic state versus time was extracted. In all cases, the decay is purely exponential suggesting a one step Néel-Brown process. In addition, the evolution of the dwell time as a function of field and current were obtained. The evolutions of the dwell times with magnetic field for either nucleation or depinning processes are in good agreement with theoretical predictions [24]. However, the influence of the current on the evolution of the dwell times for nucleation and depinning processes is not in agreement with the theory. This study suggests that the dynamic of the magnetization reversal induced by current is not fully understood and that more investigation is needed.

## References

- [1] J. Slonczewski, J. Magn. Magn. Mater. **159**, L1 (1996)
- [2] L. Berger, Phys. Rev. B **54**, 9353 (1996)
- [3] J. A. Katine et al Phys. Rev. Lett. **84**, 3149 (2000).
- [4] E. B. Myers et al Science **285**, 867 (1999).
- [5] J. A. Katine et al. J. Magn. Magn. Mater. **320**, 1217 (2008).
- [6] D. Chiba et al. Phys. Rev. Lett. **93**, 216602 (2004).
- [7] P. M. Braganca et al Appl. Phys. Lett. **87**, 112507 (2005).
- [8] O. Ozatay, et al. Nature Mater. **7**, 567 (2008).
- [9] S. Mangin, et al. Nature Mater. **5**, 210 (2006).
- [10] D. Ravelosona et al. Phys. Rev. Lett. **96**, 186604 (2006).
- [11] D. Ravelosona et al. J. Phys. D **40**, 1253 (2007).
- [12] M. Nakayama et al. J. Appl. Phys. **103** 07A710 (2008).
- [13] T. Seki, et al. Appl. Phys. Lett. **89**, 172504 (2006).
- [14] H. Meng et al. Appl. Phys. Lett. **88**, 172506 (2006).
- [15] T. Seki et al Phys. Rev. B **77**, 214414 (2008).
- [16] S. Mangin et al, Appl. Phys. Lett. **94**, 012502 (2009)
- [17] Y. Bazaliy et al. Phys. Rev. B **69**, 094421 (2004)
- [18] R. Zhu et al J. Appl. Phys. **103**, 07A722 (2008).
- [19] Y. Henry et al. Phys. Rev. B. **79** 214422 (2009)
- [20] D. Bedau, et al Appl. Phys. Lett **96** 022514 (2010)
- [21] J.Z. Sun Phys. Rev. B. **62**, 570 (2000)
- [22] See S. S. P. Parkin, M. Hayashi, L. Thomas, Science **320**, 190 (2008) and references therein.
- [23] J. Cucchiara, et al Appl. Phys. Lett. **94** 102503 (2009)
- [24] Z. Li and S. Zhang, Phys. Rev. B **69**, 134416 (2004)